JACS
JOURNAL OF THE AMERICAN CHEMICAL SOCIETY

Article

pubs.acs.org/JACS

Microwave- and Nitronium Ion-Enabled Rapid and Direct Production of Highly Conductive Low-Oxygen Graphene

Pui Lam Chiu,[†] Daniel D. T. Mastrogiovanni,[‡] Dongguang Wei,[§] Cassandre Louis,[⊥] Min Jeong,[†] Guo Yu,[†] Peter Saad,[†] Carol R. Flach,[†] Richard Mendelsohn,[†] Eric Garfunkel,[‡] and Huixin He*[,†]

[†]Chemistry Department, Rutgers University, Newark, New Jersey 07102, United States

[‡]Department of Chemistry and Chemical Biology, Rutgers University, 610 Taylor Road, Piscataway, New Jersey 08854, United States

[§]Carl Zeiss Microscopy, LLC, Thornwood, New York 10594, United States

[⊥]Irvington High School, 1253 Clinton Avenue, Irvington, New Jersey 07111, United States

Supporting Information

ABSTRACT: Currently the preferred method for large-scale production of solution-processable graphene is via a nonconductive graphene oxide (GO) pathway, which uncontrollably cuts sheets into small pieces and/or introduces nanometer-sized holes in the basal plane. These structural changes significantly decrease some of graphene's remarkable electrical and mechanical properties. Here, we report an unprecedented fast and scalable approach to avoid these problems and directly produce large, highly conductive graphene sheets. This approach intentionally excludes $KMnO_4$ from Hummers' methods and exploits aromatic oxidation by nitronium ions combined with the unique properties of microwave heating. This combination promotes rapid and simultaneous oxidation of multiple non-neighboring carbon atoms across an entire graphene sheet, thereby producing only a minimum concentration of oxygen moieties sufficient to enable the separation of graphene sheets. Thus, separated graphene sheets, which are referred to as microwave-enabled low-oxygen graphene, are thermally stable and highly conductive without requiring further reduction. Even in the absence of polymeric or surfactant stabilizers, concentrated dispersions of graphene with clean and well-separated graphene sheets can be obtained in both aqueous and organic solvents. This rapid and scalable approach produces high-quality graphene sheets of low oxygen content, enabling a broad spectrum of applications via low-cost solution processing.

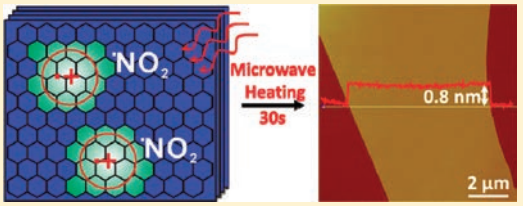

INTRODUCTION

Because of its excellent electronic, thermal, and mechanical properties, and its large surface area and low mass, graphene holds great potential for a range of applications. Fundamental studies and high-frequency electronics require pristine graphene.[1] However, "bulk" applications such as energy and hydrogen storage,[2,3] flexible macroelectronics,[4,5] and mechanically reinforced conductive coatings (including films for electromagnetic interference shielding in aerospace applications)[6−8] require large quantities of high-quality, solution-processable graphene manufactured at low cost.

Most efforts have focused on enabling mass production of solution-processable graphene through time-consuming Hummers' or modified Hummers' methods.[9−18] In brief, one must oxidize graphite powder, exfoliate the oxidized product to form nonconductive graphene oxide (GO) suspensions, and finally reduce it to recover some fraction of its electrical conductivity via thermal and/or chemical methods. These processes can lead to excessive cutting of the graphene sheets into small pieces and generate nanometer-sized holes and vacancies in the basal plane.[19,20] These holes and vacancies decrease the integrity of the material, thereby significantly altering their desired physical properties, such as molecular impermeability, electrical and thermal conductivity, and mechanical strength.[21] Furthermore, to prevent aggregation of individual graphene sheets during the reduction step, surfactants and/or stabilizers are used, resulting in graphene with species attached to both sides. Residual surfactants/stabilizers can increase the resistance between the individual sheets in a thin film, thereby dramatically decreasing the overall electrical conductivity. In addition, even though new environmentally friendly reduction protocols are being developed,[16,22] hydrazine, a hazardous material, is still widely used as the reducing agent to restore the conductivity of graphene. Finally, trace amounts of reducing agents and metal ions following Hummers' approaches can participate in unwanted reactions and be detrimental to applications such as organic solar cells.[6] Therefore, extensive cleaning and purification steps are required, making industrial-scale production expensive.

This work aims to develop a simple and scalable approach that can avoid the problems mentioned above, to quickly (30 s) and directly produce large (400−900 μm^2), clean, and highly conductive solution-processable graphene sheets without the need of a reduction process. This new approach is inspired in part by the recent atomic-level studies of the formation of

Received: November 14, 2011

   dx.doi.org/10.1021/ja210725p | J. Am. Chem. Soc. XXXX, XXX, XXX−XXX

vacancies and larger holes in graphene, the chemical cutting of graphene and carbon nanotubes (CNTs) into small pieces (see Supporting Information),[20,23−25] and the recent discoveries by Tour et al.,[26] who found that CNTs can be cut longitudinally into GO ribbons based on an alkene oxidation mechanism using $KMnO_4$. The explanation behind the anisotropic cutting was that the oxidation is initiated at defects, such as alkenes on a CNT. Further oxidation is dramatically accelerated by attacking neighboring carbon atoms, producing oxygen-containing groups next to each other. Therefore, to avoid any undesired graphene cutting, we exclude $KMnO_4$ (used in Hummers' recipe) and make full use of oxidation by nitronium ions (NO_2^+) that are produced by mixing concentrated H_2SO_4 and HNO_3.[27,28] Nitronium ions interact with a graphene surface to form multiple aromatic radical-ion pairs via a single electron transfer (SET) pathway (see Supporting Information).[29] At higher temperatures, multiple −OH and/or epoxy groups can be formed across the graphene surface following oxygen transfer to the aromatic radicals (Figure 1a).[27] Due to the electron-donating capability of the resulting −OH and epoxy groups, subsequent oxidation results in more −OH and epoxy groups that are preferentially formed far away from the already oxidized carbon atoms.[28] This is in contrast to $KMnO_4$, which preferentially attacks adjacent carbon atoms. An important consequence is that the initial oxidation by NO_2^+ can naturally produce intact graphene domains separated by regions of oxygen-containing groups. However, if the reaction does not stop in a timely manner, subsequent oxidation will lead to the formation of oxides, vacancies, larger holes,[25] and ultimately cutting of the graphene into small pieces, analogous to what was shown in previous CNT cutting studies.[23,24] Therefore, the key to directly produce large, conductive graphene sheets by NO_2^+ is to quickly produce the low concentration of oxygen moieties that is required for the separation of individual graphene sheets, and then quench the reaction before holes and/or vacancies form (see Supporting Information). Microwave heating satisfies these requirements. Due to the high conductivity and polarizability of graphene (and graphite), the local temperature can be significantly increased (under microwave irradiation), which in turn leads to higher oxidation rates. Furthermore, movement of the intercalation agent, H_2SO_4, and the oxidant, NO_2^+, is also dramatically increased upon microwave irradiation due to their ionic nature.[30] These concerted processes lead to the rapid dispersion of large graphene sheets containing a minimal amount of oxygen. Due to the essential role of microwave heating during the production, we refer to these graphene sheets as microwave-enabled low-oxygen graphene (ME-LOGr). Compared to reduced graphene oxide (rGO) sheets prepared using Hummers' method, the ME-LOGr sheets exhibit much larger sizes (400−900 μm^2), fewer defects, greater thermal stability, and conductivity comparable to or higher than that of the solution-processable graphene reported in the literature. Our approach also results in graphene capable of being dispersed in either aqueous or organic solvents without the need of stabilizers.

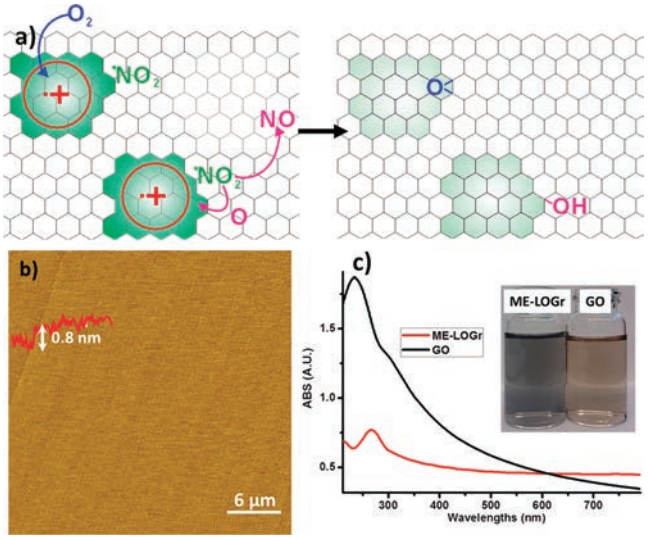

Figure 1. (a) Schematic drawing showing the proposed oxidation mechanism to directly produce highly conductive, low-oxygen-containing amphiphilic graphene sheets. A nitronium ion forms a single electron transfer (SET) intermediate with a graphene layer, which is intercepted by a rapid oxygen transfer from molecular oxygen, affording an epoxy group, or from NO_2^+ to form an OH group. (b) AFM image of a large ME-LOGr sheet deposited on a freshly cleaved mica surface. (c) UV−vis spectra of ME-LOGr (red) and GO (black). Inset: digital photograph showing the different colorations of ME-LOGr and GO solutions in water.

RESULTS AND DISCUSSION

In a typical experiment, graphite powder is mixed with concentrated sulfuric acid and nitric acid (1:1 volume ratio) and then subjected to 30 s of microwave irradiation (300 W). The reaction results in a finely dispersed suspension that is significantly easier to purify and handle than the sticky paste obtained from Hummers' method.[31] A colloidal graphene solution is obtained through direct dialysis of this suspension. Atomic force microscopy (AFM), scanning electron microscopy (SEM), and scanning transmission electron microscopy (STEM) reveal that the lateral size of the single graphene sheets is on average 20−30 μm (400−900 μm^2), which is the size of the starting graphite powder (Figure 1b, and Supporting Information, Figure S1a−c). The large size of the resulting graphene sheets suggests that no unintentional cutting occurs during the short microwave irradiation (30 s). Graphene powder can be obtained by vacuum filtration which can then be redispersed in polar solvents such as water or *N*,*N*-dimethylformamide (DMF) to form colloidal solutions (demonstrated by the Tyndall effect, Supporting Information, Figure S2) with concentrations up to 3 mg/mL. In a nonpolar solvent, such as dichloroethene, suspensions possessing concentrations of 20 mg/L are achievable with the help of bath sonication or magnetic stirring. The high dispersibility in both polar and nonpolar solvents without requiring surfactants or stabilizers indicates the amphiphilic nature of ME-LOGr, which is quite different from previously reported graphene sheets.[32] These solutions are stable and exhibit no precipitation for several months. Even though the sizes of the graphene sheets were slightly reduced (several to tens of micrometers) after mechanical stirring, their size remains significantly larger than that of GO sheets (hundreds of nanometers) prepared by Hummers' method (Supporting Information, Figure S3).[9] We did not observe holes in the ME-LOGr sheets, in contrast to the graphene sheets dispersed in the presence of pyrene derivatives.[18] However, increasing the microwave irradiation time to 60 s caused a significant decrease in the size of the sheets, possibly due to overoxidation-induced cutting and etching (Supporting Information, Figure S4).[23]

dx.doi.org/10.1021/ja210725p | *J. Am. Chem. Soc.* XXXX, XXX, XXX−XXX

The color of ME-LOGr suspensions is grayish-black, which qualitatively suggests that we have directly obtained electrically conductive graphene sheets instead of the typically brown GO solutions (Figure 1c, inset).[12,13] A control experiment was performed by adding a small amount of $KMnO_4$ to the HNO_3/H_2SO_4 acid mixture. This yielded a bright yellow solution of fully oxidized GO (Supporting Information, Figure S5), demonstrating the importance of excluding $KMnO_4$ in our procedure. Additionally, unlike GO, the UV−vis−near-IR spectrum of the ME-LOGr solution displayed an absorption maximum at 267 nm and relatively uniform absorption in the visible and NIR regions (Figure 1c), which suggests that the π-conjugation within the graphene sheets is largely retained.[12,14,33] However, when conventional (instead of microwave) heating was used, a fully oxidized GO was obtained, demonstrating the utility of microwave irradiation.

Figure 2 shows the Raman spectra of ME-LOGr and GO films deposited on alumina membranes. The typical features of

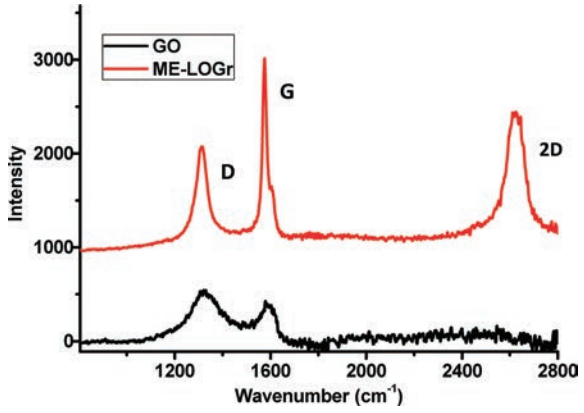

Figure 2. Raman spectra of ME-LOGr (red) and GO (black). The small intensity ratio of D/G bands and the high intensity of the 2D band in ME-LOGr are in contrast to the larger D/G band ratio and the absence of a 2D band in GO, indicating ME-LOGr has more ideal graphitic structures without adsorbent-induced surface modification.

the G band, defect D band, and 2D band are shown in the Raman spectrum of ME-LOGr. The D-to-G band intensity ratio (I_D/I_G) is 0.45 and 1.23 for ME-LOGr and GO, respectively. Using the empirical Tuinstra−Koenig relation,[34] we found that the size of the ordered crystallite graphitic domains was ~10 nm in ME-LOGr, while the domain size in GO was ~3.5 nm. The reported I_D/I_G ratios for rGO are similar to or even higher than those for GO, which was explained by the fact that chemical reduction preferentially generates a greater number of smaller crystalline domains rather than increasing the size of existing graphitic domains.[13,16] Therefore, though the apparent electronic structure of the ME-LOGr sheets is similar to that of rGO, as demonstrated by its color and UV−vis spectrum, the ME-LOGr sheets have unique molecular structures that differ from both GO and rGO.[13,35]

The 2D band in GO is absent, which is consistent with previous reports.[9,13] Additionally, the literature states that reduction of GO results in only a small increase in the 2D band due to the defects in the graphitic structures.[16] A decrease of the 2D band is also associated with the modification of pristine graphene through chemisorption[36] and physisorption.[15,37] However, for ME-LOGr the intensity of the 2D band is similar to that of the G band, demonstrating a more ideal structure without adsorbent-induced surface modification.[16]

To further understand the structure of the ME-LOGr on an atomic level, we used low-voltage aberration-corrected high-resolution transmission electron microscopy (HRTEM) to carefully examine the structure of the ME-LOGr sheets and compare them to what was observed for GO and rGO.[19,38] Both GO and rGO contain nearly perfect graphene domains ranging from 1 to 3 nm, separated by amorphous-like regions and nanometer-sized holes. Additionally, rGO appears to be more sensitive to the electron beam than GO during TEM imaging. Similar to GO and rGO, ME-LOGr also exhibits multiple crystalline-like domains connected by amorphous regions. However, the ME-LOGr structure remained stable during imaging, and no nanometer-sized holes were observed (Figure 3; see also Supporting Information, Figure S6), in agreement with the AFM data. The crystalline domains are on the order of 6−10 nm across, larger than those observed for GO and rGO, and are consistent with the Raman study.

The chemical functionalities of the ME-LOGr sheets were studied using X-ray photoelectron spectroscopy (XPS) and Fourier transform infrared spectroscopy (FTIR). The C 1s core-level XPS spectra of ME-LOGr and GO show a main peak of oxygen-free carbon (see Supporting Information) and a shoulder of oxygen-containing carbon (Figure 4a). The oxygen-free carbon of ME-LOGr makes up 79% of the spectrum, comparable to the spectrum of reduced GO,[42] whereas the spectrum of GO (Figure 4b) contains an oxygen-free carbon signal that is 49% of the total carbon signal, which is much lower than that in ME-LOGr. Measurements by Rutherford backscattering spectrometry (RBS) show that ME-LOGr exhibits almost an order of magnitude lower oxygen content than that observed in GO films (C:O ratios of 25:1 and 3:1, respectively), consistent with the XPS study. Neither of these two techniques detected nitrogen or sulfur signals in the films, suggesting that no nitration or sulfonation occurred.[39] The XPS contribution from the oxidized carbon species in ME-LOGr is in agreement with FTIR data that identifies the majority of the functional groups as alcohol and epoxide (Supporting Information, Figure S7). ME-LOGr contains a very small amount of carbonyl-containing groups, in contrast to GO. This further illustrates the different oxidation mechanisms of NO_2^+ and $KMnO_4$.

The thermal stability of as-prepared ME-LOGr sheets was compared to those of GO and the parent graphite powder using thermal gravimetric analysis (TGA) (Figure 5a). Below 100 °C, the major mass loss has been assigned to desorption of water molecules, even though a complete desorption of water may need higher temperatures.[25] The high concentration of water in GO has been reported to be the result of the high density of oxygen-containing functionalities (including hydroxyl).[40] The minor mass loss of ME-LOGr in this temperature range indicates that the material exhibits only a weak interaction with water, behaving similar to the parent graphite powder. At higher temperatures, GO continues losing mass, presumably due to pyrolysis of the labile, oxygen-containing functional groups.[25,41,42] The sharp mass loss that occurred around 200−300 °C has been assigned to pyrolysis of hydroxyl, epoxide, and carboxyl groups.[43,44] The low weight loss in these temperature ranges further suggests the low concentration of hydroxyl, epoxide, and carboxyl groups in the ME-LOGr sheets, which is consistent with the XPS results. The sharp mass loss above 500 °C has been ascribed to the combustion of carbon in the

dx.doi.org/10.1021/ja210725p | J. Am. Chem. Soc. XXXX, XXX, XXX−XXX

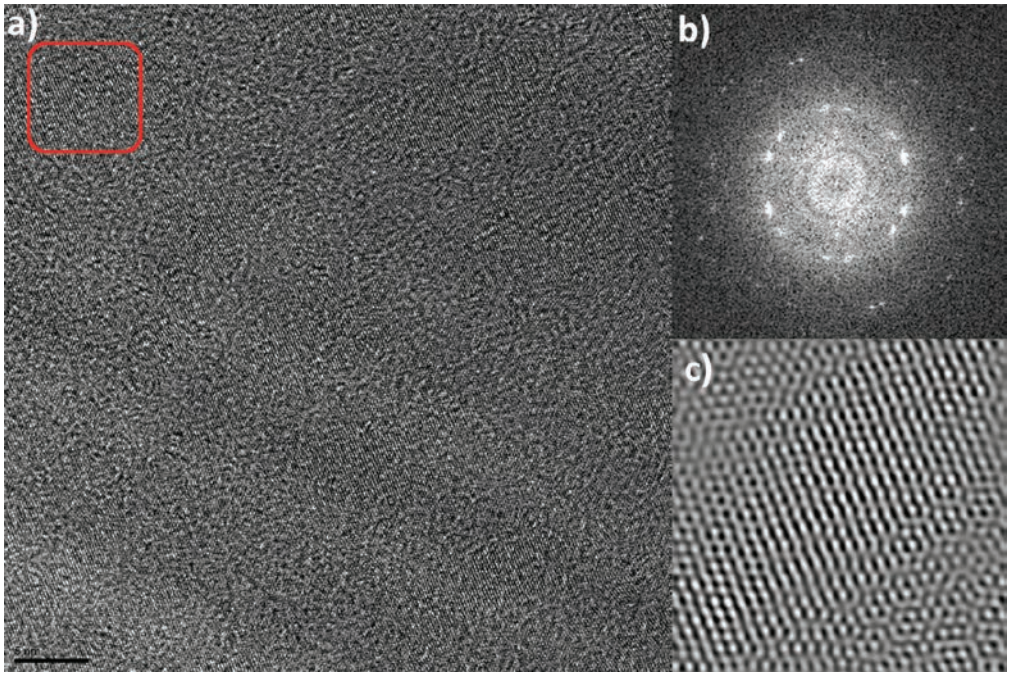

Figure 3. (a) Representative HRTEM image of ME-LOGr, which is composed of many different crystalline-like domains with average lateral size of 6−10 nm. No nanometer-sized holes were observed, which is highly in contrast to GO and rGO. The size of the crystalline domains is also much larger than those observed in GO and rGO. (b) Fast Fourier transform (FFT) pattern of the selected region indicated in (a). (c) The reconstructed image of the same spot as (b) after filtering with the frequency domain to include contributions from both sets of hexagons of the FFT pattern. The scale bar in (a) is 5 nm.

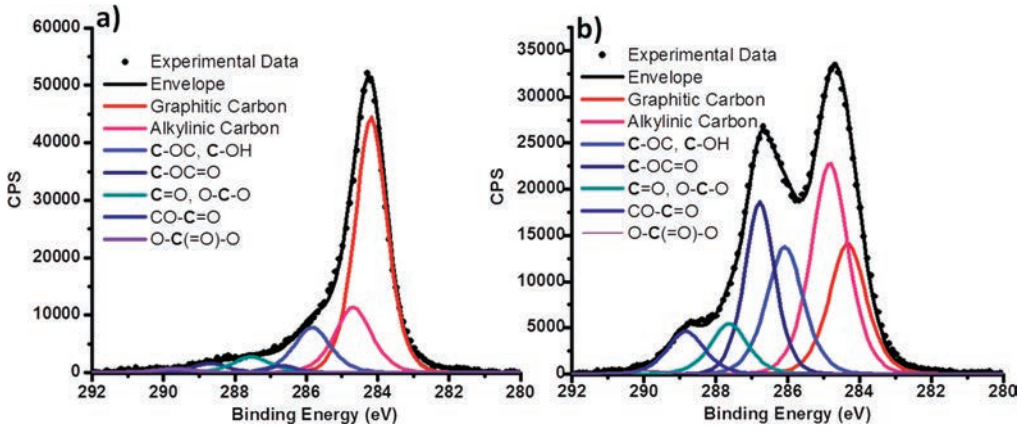

Figure 4. Carbon 1s core XPS spectra for thin films of (a) ME-LOGr and (b) GO. The content of oxygen-free carbon of ME-LOGr was 79%, which was comparable with the reported value of fully reduced GO, while GO (b) contains only 49% of oxygen-free carbon. This is direct evidence of much less oxidation in the ME-LOGr.

graphene backbone.[45] It is interesting to note that even though the rate of mass loss of GO and ME-LOGr was similar between 300 and 500 °C, the complete combustion for ME-LOGr happens at a higher temperature than that of GO. This result indicates that the ME-LOGr may have better thermal stability than thermally reduced GO sheets.

Recently, the evolution of carbon bonds in GO thin films has been carefully studied by monitoring XPS and IR differential spectra as a function of annealing temperatures.[25,41,42] Thermal annealing of GO has been shown to result in removal of the entrapped water molecules and the epoxide and hydroxyl groups by formation of H_2O, H_2, O_2, CO, and CO_2, thus creating defects in the form of etched holes within the graphene basal plane.[46] Zettl et al. reported on the existence of a large number of holes and vacancies in rGO, obtained by a combination of chemical and thermal reduction. They found that the presence of these defects dramatically decreases the stability of rGO to the electron beam during TEM imaging.[19] The higher thermal stability of the ME-LOGr is consistent with the TEM observation that the structure of ME-LOGr is stable during imaging and contains no holes and fewer defects.

We prepared graphene films of different thicknesses from the ME-LOGr suspensions by vacuum filtration through an anodic filter membrane.[9] The electrical properties of the graphene sheets without any chemical or thermal reduction processes were studied by measuring the sheet resistance of the corresponding graphene films with a four-probe approach. Similar to other methods that utilize graphene sheets dispersed in solutions, the ME-LOGr films show percolation-type electronic behavior. The sheet resistance of the ME-LOGr

dx.doi.org/10.1021/ja210725p | J. Am. Chem. Soc. XXXX, XXX, XXX−XXX

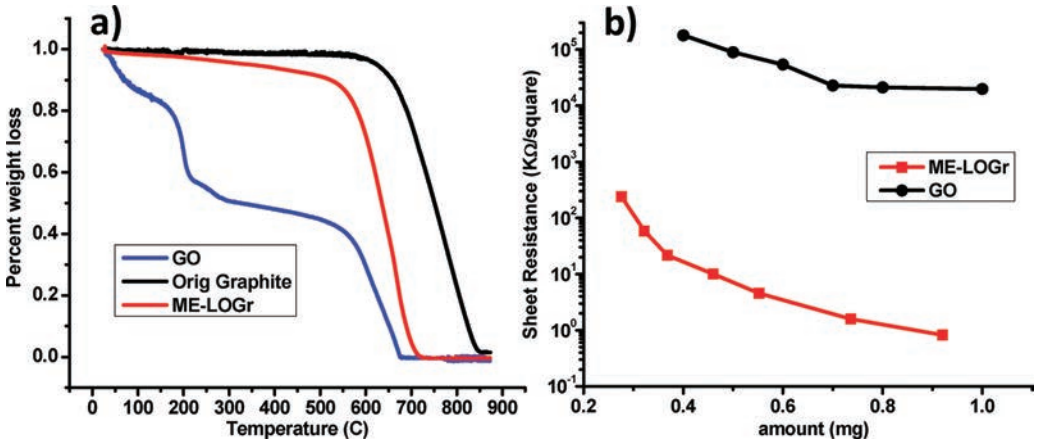

Figure 5. (a) TGA curves of % weight loss plotted against temperature, showing that ME-LOGr (red) is thermally much more stable than GO (blue) and highly comparable with its parent graphite (black). (b) Percolation study of ME-LOGr and GO using a four-point probe setup. After percolation threshold, the sheet resistivity of ME-LOGr (red) is 5 orders of magnitude lower than that of the heavily oxidized GO films.

film decreases with increasing film thickness, as shown in Figure 5b. After reaching the percolation threshold, the sheet resistance of the ME-LOGr film is 1.0 kΩ/square. To estimate the DC conductivity of the film, a filtered ME-LOGr film was divided to two parts. One part was transferred onto a quartz substrate for conductivity measurement, and the other half was transferred onto a beryllium substrate to precisely measure the thickness of the film (see detail in Supporting Information). The sheet resistance was measured to be 0.76 kΩ/square, and the thickness of the film was 200 nm. This corresponds to a DC conductivity of 6600 S m^{-1}. It is worth mentioning that this conductivity was achieved on the as-prepared film which had been neither chemically nor thermally reduced. This conductivity is much higher than that of graphene sheets directly exfoliated in the presence of surfactants/stabilizers, even though they were known to have a low density of defects. For instance, graphene sheets dispersed in sodium dodecylbenzene sulfonate have a DC conductivity of 35 S m^{-1}.[15] Recently, we reported that the DC conductivity of the graphene sheets dispersed in the presence of pyrene derivatives before thermal annealing was around 1900 S m^{-1}.[18] The conductivity of the as-produced ME-LOGr is much more comparable to that of surfactant-free reduced GO sheets obtained by hydrazine reduction under basic conditions (DC conductivity of 7200 S m^{-1}).[12] We believe that the high conductivity is due to the high conductivity as well as the relative cleanliness (nonfunctionalization) of the individual ME-LOGr sheets, which enables low intersheet contact resistance. It is known that directly exfoliating graphite in certain organic solvents, such as *N*-methylpyrrolidone (NMP), can produce graphene sheets with not only a low density of defects but also clean surfaces without any surfactants or stabilizers. However, these solvents are expensive, require special care, tend to have high boiling points, and are difficult to completely remove. Residual solvent also results in poor electronic contacts between graphene sheets and therefore lowers the overall conductivity of the resulting multisheet graphene films. It was reported that the as-produced film has a conductivity of 5 S m^{-1}.[14] After thermal annealing at 300 °C for 2 h, a conductivity of 5000 S m^{-1} was achieved. With annealing in a reductive environment (Ar/H_2) at 250 °C for 2 h, a slightly higher conductivity of 6500 S m^{-1} was achieved.[14] Upon annealing a ME-LOGr film at 300 °C in Ar for 2 h to remove some of the oxygen-containing groups, the conductivity was increased to 19 200 S m^{-1}, significantly higher than that of films prepared via graphene dispersed by NMP- and hydrazine-reduced GO in basic conditions.

We emphasize that microwave methodologies are easy to scale and do not suffer from thermal gradient effects, providing a potentially industrially important improvement over convective methods.[30] Microwave irradiation was also exploited for other graphene research projects. For example, it has been applied to fabricate exfoliated graphite (EG) from a wide range of graphite intercalation compounds (GIC),[47] simultaneous exfoliation and reduction of GO,[48] and simultaneous intercalation and exfoliation of graphite powder.[49] However, this is the first report that large, clean, and highly conductive graphene of an intrinsically amphiphilic nature can be directly and rapidly produced with high yield.

■ CONCLUSION

An unprecedented fast and scalable approach has been developed to directly produce large, highly conductive graphene sheets. This method has the following advantages for mass production: (1) short production periods (30 s), (2) much larger sheet size (400−900 μm^2), (3) fewer destructive defects such as nanometer-sized holes, (4) high-concentration dispersions in both aqueous and organic solvents (without requiring polymeric or surfactant stabilizers), (5) fewer starting materials and low cost (compared to commonly used Hummers' and modified Hummers'), and (6) reduced waste from purification steps. This process can enable a broad range of real-world applications to be realized using solution processing.

■ METHODS

The graphite used for all experiments was synthetic graphite (~20 μm, Sigma-Aldrich), used as received. To fabricate ME-LOGr, 20 mg of synthetic graphite powder was added and mixed into a solution of sulfuric acid and nitric acid (ratio of 1:1 with a total volume of 10 mL) in a round-bottom flask. The flask was exposed to 30 s of 300 W microwave irradiation in a CEM Discover microwave reactor. For the reaction with $KMnO_4$, 0.65 g of $KMnO_4$ was also added into the reaction at this step. A colloidal graphene solution was obtained by directly dialysis of the suspension, which largely avoided mechanical agitation of the sheets. Before dialysis, the suspension was first neutralized in an ice-bath using 4 M KOH until pH values were close to 7. For a quick cleanup process, the whole content was then filtered

dx.doi.org/10.1021/ja210725p | J. Am. Chem. Soc. XXXX, XXX, XXX−XXX

through an Anodisc aluminum filter membrane with 0.2 μm pore size, and the filtrate was washed with 600 mL of deionized water. Graphene colloidal solution was obtained by bath sonication or magnetic stirring of the filtrate, followed by centrifugation at 4000 rpm for 20 min to remove any unexfoliated graphite powder. GO was fabricated using a modified Hummers' method.[31]

Absorption spectra were recorded on a Cary 500 UV−vis−NIR spectrophotometer in double-beam mode using 1 cm quartz cuvettes. Samples for AFM (Veeco Nanoscope IIIa) and micro-Raman spectroscopy (Kaiser Optical Systems Raman Microprobe equipped with a 785 nm solid-state diode laser) were prepared by dip-coating or drop-casting on freshly cleaved mica (AFM) and a 300 nm SiO_2-on-Si wafer, respectively. TGA was performed with a nitrogen flow (20 mL/min) using a Perkin-Elmer Thermogravimetric Analyzer Pyris 1 on sample sizes of about 2−3 mg. The furnace was heated from room temperature to 1000 at 5 °C/min. HRTEM investigations were carried out with a beam energy of 80 kV using a Zeiss 200 kV Cs-corrected Libra 200 FEG energy-filtering TEM. X-ray photoelectron spectroscopy was performed using a Thermo Scientific K-Alpha instrument, and data were analyzed using CasaXPS 2.3.15 software (see Supporting Information). All solutions were prepared using deionized water (18.2 MΩ) (Nanopure water, Barnstead), which was also used to rinse and clean the samples. Sheet resistance measurements were determined by a manual four-point resistivity probe (Lucas Laboratories, model 302) on graphene films prepared by vacuum filtration using Anodisc 47 inorganic membranes (200 nm pores; Whatman Ltd.). After filtration, the thin films were dried in air for 15−20 min.

■ ASSOCIATED CONTENT

Supporting Information

Additional discussion, detailed experimental procedures, and complete ref 14. This material is available free of charge via the Internet at http://pubs.acs.org.

■ AUTHOR INFORMATION

Corresponding Author

huixinhe@newark.rutgers.edu

Notes

The authors declare no competing financial interest.

■ ACKNOWLEDGMENTS

This material is based upon work supported by the National Science Foundation under Grants CHE-0750201, CBET-0933966, MRI-1039828 (P.C. and H.H.), and DMR 1006740 (E.G. and D.M.). We also acknowledge Manish Chhowalla, Eva Andrei, Hisato Yamaguchi, Rajesh Kappera, and Ivan Skachko for helpful discussions, and Leszek Weilunski for RBS measurements.

■ REFERENCES

(1) Wu, Y. Q.; Lin, Y. M.; Bol, A. A.; Jenkins, K. A.; Xia, F. N.; Farmer, D. B.; Zhu, Y.; Avouris, P. *Nature* **2011**, *472*, 74.

(2) Zhu, Y.; Murali, S.; Stoller, M. D.; Ganesh, K. J.; Cai, W.; Ferreira, P. J.; Pirkle, A.; Wallace, R. M.; Cychosz, K. A.; Thommes, M.; Su, D.; Stach, E. A.; Ruoff, R. S. *Science* **2011**, *332*, 1537.

(3) Jin, Z.; Lu, W.; O'Neill, K. J.; Parilla, P. A.; Simpson, L. J.; Kittrell, C.; Tour, J. M. *Chem. Mater.* **2011**, *23*, 923.

(4) Eda, G.; Chhowalla, M. *Adv. Mater.* **2010**, *22*, 2392.

(5) Wobkenberg, P. H.; Eda, G.; Leem, D. S.; de Mello, J. C.; Bradley, D. D. C.; Chhowalla, M.; Anthopoulos, T. D. *Adv. Mater.* **2011**, *23*, 1558.

(6) Dubin, S.; Gilje, S.; Wang, K.; Tung, V. C.; Cha, K.; Hall, A. S.; Farrar, J.; Varshneya, R.; Yang, Y.; Kaner, R. B. *ACS Nano* **2010**, *4*, 3845.

(7) Stankovich, S.; Dikin, D. A.; Dommett, G. H. B.; Kohlhaas, K. M.; Zimney, E. J.; Stach, E. A.; Piner, R. D.; Nguyen, S. T.; Ruoff, R. S. *Nature* **2006**, *442*, 282.

(8) Ramanathan, T.; Abdala, A. A.; Stankovich, S.; Dikin, D. A.; Herrera-Alonso, M.; Piner, R. D.; Adamson, D. H.; Schniepp, H. C.; Chen, X.; Ruoff, R. S.; Nguyen, S. T.; Aksay, I. A.; Prud'homme, R. K.; Brinson, L. C. *Nature Nanotechnol.* **2008**, *3*, 327.

(9) Eda, G.; Fanchini, G.; Chhowalla, M. *Nature Nanotechnol.* **2008**, *3*, 270.

(10) Behabtu, N.; Lomeda, J. R.; Green, M. J.; Higginbotham, A. L.; Sinitskii, A.; Kosynkin, D. V.; Tsentalovich, D.; Parra-Vasquez, A. N. G.; Schmidt, J.; Kesselman, E.; Cohen, Y.; Talmon, Y.; Tour, J. M.; Pasquali, M. *Nature Nanotechnol.* **2010**, *5*, 406.

(11) Li, X. L.; Zhang, G. Y.; Bai, X. D.; Sun, X. M.; Wang, X. R.; Wang, E.; Dai, H. J. *Nature Nanotechnol.* **2008**, *3*, 538.

(12) Li, D.; Muller, M. B.; Gilje, S.; Kaner, R. B.; Wallace, G. G. *Nature Nanotechnol.* **2008**, *3*, 101.

(13) Tung, V. T.; Allen, M. J.; Yang, Y.; Kaner, R. B. *Nature Nanotechnol.* **2009**, *4*, 25.

(14) Hernandez, Y.; et al. *Nature Nanotechnol.* **2008**, *3*, 563.

(15) Lotya, M.; Hernandez, Y.; King, P. J.; Smith, R. J.; Nicolosi, V.; Karlsson, L. S.; Blighe, F. M.; De, S.; Wang, Z.; McGovern, I. T.; Duesberg, G. S.; Coleman, J. N. *J. Am. Chem. Soc.* **2009**, *131*, 3611.

(16) Moon, I. K.; Lee, J.; Ruoff, R. S.; Lee, H. *Nature Commun.* **2010**, *1*, 73.

(17) Wang, J. Z.; Manga, K. K. M.; Bao, Q. L.; Loh, K. P. *J. Am. Chem. Soc.* **2011**, *133*, 8888.

(18) Zhang, M.; Parajuli, R. R.; Mastrogiovanni, D.; Dai, B.; Lo, P.; Cheung, W.; Brukh, R.; Chiu, P. L.; Zhou, T.; Liu, Z. F.; Garfunkel, E.; He, H. X. *Small* **2010**, *6*, 1100.

(19) Erickson, K.; Erni, R.; Lee, Z.; Alem, N.; Gannett, W.; Zettl, A. *Adv. Mater.* **2010**, *22*, 4467.

(20) Li, J.-L.; Kudin, K. N.; McAllister, M. J.; Prud'homme, R. K.; Aksay, I. A.; Car, R. *Phys. Rev. Lett.* **2006**, *96*, 176101.

(21) Geim, A. K. *Science* **2009**, *324*, 1530.

(22) Zhu, C. Z.; Guo, S. J.; Fang, Y. X.; Dong, S. J. *ACS Nano* **2010**, *4*, 2429.

(23) Ziegler, K. J.; Gu, Z. N.; Peng, H. Q.; Flor, E. L.; Hauge, R. H.; Smalley, R. E. *J. Am. Chem. Soc.* **2005**, *127*, 1541.

(24) Liu, J.; Rinzler, A. G.; Dai, H. J.; Hafner, J. H.; Bradley, R. K.; Boul, P. J.; Lu, A.; Iverson, T.; Shelimov, K.; Huffman, C. B.; Rodriguez-Macias, F.; Shon, Y. S.; Lee, T. R.; Colbert, D. T.; Smalley, R. E. *Science* **1998**, *280*, 1253.

(25) Bagri, A.; Mattevi, C.; Acik, M.; Chabal, Y. J.; Chhowalla, M.; Shenoy, V. B. *Nature Chem.* **2010**, *2*, 581.

(26) Kosynkin, D. V.; Higginbotham, A. L.; Sinitskii, A.; Lomeda, J. R.; Dimiev, A.; Price, B. K.; Tour, J. M. *Nature* **2009**, *458*, 872.

(27) Esteves, P. M.; Carneiro, J. W. D.; Cardoso, S. P.; Barbosa, A. G. H.; Laali, K. K.; Rasul, G.; Prakash, G. K. S.; Olah, G. A. *J. Am. Chem. Soc.* **2003**, *125*, 4836.

(28) de Queiroz, J. F.; Carneiro, J. W. D.; Sabino, A. A.; Sparrapan, R.; Eberlin, M. N.; Esteves, P. M. *J. Org. Chem.* **2006**, *71*, 6192.

(29) Loughin, S.; Grayeski, R.; Fischer, J. E. *J. Chem. Phys.* **1978**, *69*, 3740.

(30) *Microwave-Enhanced Chemistry: Fundamentals, Sample Preparation, and Applications*; Kingston, H. M., Haswell, S. J., Eds.; American Chemical Society: Washington, DC, 1997.

(31) Hummers, W. S.; Offeman, R. E. *J. Am. Chem. Soc.* **1958**, *80*, 1339.

(32) Qi, X. Y.; Pu, K. Y.; Li, H.; Zhou, X. Z.; Wu, S. X.; Fan, Q. L.; Liu, B.; Boey, F.; Huang, W.; Zhang, H. *Angew. Chem., Int. Ed.* **2010**, *49*, 9426.

(33) Becerril, H. A.; Mao, J.; Liu, Z. F.; Stoltenberg, R. M.; Bao, Z.; Chen, Y. S. *ACS Nano* **2008**, *2*, 463.

(34) Tuinstra, F.; Koenig, J. L. *J. Chem. Phys.* **1970**, *53*, 1126.

(35) Wang, H. L.; Robinson, J. T.; Li, X. L.; Dai, H. J. *J. Am. Chem. Soc.* **2009**, *131*, 9910.

(36) Niyogi, S.; Bekyarova, E.; Itkis, M. E.; Zhang, H.; Shepperd, K.; Hicks, J.; Sprinkle, M.; Berger, C.; Lau, C. N.; Deheer, W. A.; Conrad, E. H.; Haddon, R. C. *Nano Lett.* **2010**, *10*, 4061.
(37) Farmer, D. B.; Golizadeh-Mojarad, R.; Perebeinos, V.; Lin, Y. M.; Tulevski, G. S.; Tsang, J. C.; Avouris, P. *Nano Lett.* **2009**, *9*, 388.
(38) Gómez-Navarro, C.; Meyer, J. C.; Sundaram, R. S.; Chuvilin, A.; Kurasch, S.; Burghard, M.; Kern, K.; Kaiser, U. *Nano Lett.* **2010**, *10*, 1144.
(39) Wang, Y. B.; Iqbal, Z.; Mitra, S. *J. Am. Chem. Soc.* **2006**, *128*, 95.
(40) Acik, M.; Mattevi, C.; Gong, C.; Lee, G.; Cho, K.; Chhowalla, M.; Chabal, Y. J. *ACS Nano* **2010**, *4*, 5861.
(41) Acik, M.; Lee, G.; Mattevi, C.; Chhowalla, M.; Cho, K.; Chabal, Y. J. *Nat. Mater.* **2010**, *9*, 840.
(42) Mattevi, C.; Eda, G.; Agnoli, S.; Miller, S.; Mkhoyan, K. A.; Celik, O.; Mastrogiovanni, D.; Granozzi, G.; Garfunkel, E.; Chhowalla, M. *Adv. Funct. Mater.* **2009**, *19*, 2577.
(43) Kittaka, S.; Fukuhara, N.; Sumida, H. *J. Chem. Soc., Faraday Trans.* **1993**, *89*, 3827.
(44) Boehm, H. P. *Carbon* **2002**, *40*, 145.
(45) Jeong, H. K.; Jin, M. H.; So, K. P.; Lim, S. C.; Lee, Y. H. *J. Phys. D, Appl. Phys.* **2009**, *42*, xx.
(46) Jung, I.; Field, D. A.; Clark, N. J.; Zhu, Y. W.; Yang, D. X.; Piner, R. D.; Stankovich, S.; Dikin, D. A.; Geisler, H.; Ventrice, C. A.; Ruoff, R. S. *J. Phys. Chem. C* **2009**, *113*, 18480.
(47) Luo, Z. T.; Lu, Y.; Somers, L. A.; Johnson, A. T. C. *J. Am. Chem. Soc.* **2009**, *131*, 898.
(48) Zhu, Y. W.; Murali, S.; Stoller, M. D.; Velamakanni, A.; Piner, R. D.; Ruoff, R. S. *Carbon* **2010**, *48*, 2118.
(49) Sridhar, V.; Jeon, J. H.; Oh, I. K. *Carbon* **2010**, *48*, 2953.